



Available online at <http://scik.org>

J. Math. Comput. Sci. 11 (2021), No. 2, 2153-2173

<https://doi.org/10.28919/jmcs/5499>

ISSN: 1927-5307

OPTIMAL NEIGHBORING INFECTION CONTROL STRATEGY ON A MULTI-REGIONS-BASED SIR EPIDEMIC MODEL

SARA BIDAHA^{1,*}, MUSTAPHA LHOUS², HAMZA BOUTAYEB¹, OMAR ZAKARY¹, MOSTAFA RACHIK¹

¹Laboratory of Analysis, Modeling and Simulation, Department of Mathematics and Computer Science, Hassan II University of Casablanca, Faculty of Sciences Ben M'Sik, Sidi Othman, BP 7955, Casablanca, Morocco

²Laboratory of Modeling, Analysis, Control and Statistics, Department of Mathematics and Computer Science, Faculty of Sciences Ain Chock, Hassan II University of Casablanca, B.P 5366 Maarif Casablanca, Morocco

Copyright © 2021 the author(s). This is an open access article distributed under the Creative Commons Attribution License, which permits unrestricted use, distribution, and reproduction in any medium, provided the original work is properly cited.

Abstract. In this article, we consider a discrete-time multiregional SIR model that describes the evolution of an epidemic in several geographic areas believed to be linked by its population movement. Therefore, those affected can spread the disease by traveling from one region to another. In this work, we aim to define a new control (vaccination) strategy that is implemented in one patch (control source patch) and helps reduce infections and increase the number of individuals recovered in another patch (target patch), and this at an optimal cost. Optimal control problems are obtained based on a discrete version of Pontryagin's maximum principle, and then determined numerically using a discrete progressive-regressive scheme that converges as a result of a practical test related to the Forward-Backward Sweep Method (FBSM) on optimal control.

Keywords: discrete-time; SIR epidemic model; multi-regions; optimal control; regional control.

2010 AMS Subject Classification: 37C75, 92B05.

*Corresponding author

E-mail address: sarabidah@gmail.com

Received January 30, 2021

1. INTRODUCTION

The mathematical modeling of the spread of infectious diseases has become part of epidemiology strategies decision-making in many countries (see [1, 2, 3, 4, 5, 6]). They can supply an efficient tool to study the dynamics and control of infectious diseases. In the history of all these diseases, we can notice their spread from one region to another, and recently the COVID-19 pandemic from its epicenter of Wuhan in China has spread to all parts of the world, which makes taking into account the spatial spread of diseases more important during modeling processes. In a wide geographical area, the disease becomes mobile because of the people's movements between regions, and the transmission network of the disease becomes more complex when people use inter-continental transport means.

Before the identification of the disease, the infected people would move from one region to another. After diagnosing some infected cases and identifying the disease in some areas, It may take time for a responsive decision to restrict all travel to and from the affected areas. At that time, the affected cases had already been distributed in many other regions, making the problem even more complicated. Different epidemic diseases have been recognized in recent decades and have spread to a large geographic area, such as HIV/AIDS [7], Ebola [8, 9, 10], Cholera [11, 12, 13], Malaria [14, 15] and Influenza [16, 17, 18] and recently, the COVID-19 [19, 20, 21]. To control the spatial spread of the disease, it became necessary to consider all the parts that people can visit. Hence, the utility of spatial dynamics in the mathematical models of the propagation of infectious diseases.

Optimal control theory is well used as an available and effective option for decision-makers to develop and simulate control strategies, see [16, 18, 22, 23], but there are very few applications with both space and time as discrete variables. Some authors have addressed the case of the epidemic model in discrete-time in the last decades, (see [24], [25], [26] and [27]). One reason for choosing discrete epidemic models is that the discrete model has the advantage of describing an infectious disease from the epidemic data that are usually collected in discrete time units.

In this work, we propose a new modeling and control approach based on multi-region discrete-time SIR (Susceptible - Infected - Removed) model to investigate the control of the spatiotemporal spread of an epidemic that emerges in several geographical regions, consequently to show the

influence existing between regions via infection connections, and to seek a reasonable control strategy which could be effective for the prevention of infectious diseases such as HIV/AIDS, Ebola, and COVID-19, or pandemics in general. We suppose that all regions are connected, and the infected people have access to all these regions. Generally, in the case of distant regions, the infection travels to a targeted region if there exists a direct or indirect mode of transport between it and the regions from where the epidemic starts. In this direction, we present a new epidemic modeling approach in where the studied area is represented by a grid of cells uniform in size, and each cell represents a region (towns, neighboring, ...).

We assume that there is an important part (patch: a set of regions) within the domain studied, that needs to be protected against the disease, and controlling its number of infected people is a higher priority, this part is called the target patch. It is assumed also that there is no way to introduce the control campaigns directly in such places, due to the sensitivity of the social group of people residing in these locations, for example, disseminating information about the infection in the district of doctors and nurses, can lead to a serious panic in the society.

To show the influence of each region on the other, we study here the effects of the vaccination on the neighborhood of a control source patch (important and/or sensitive regions). To do this, we propose this new approach that determines an optimal control based on the multi-region discrete SIR model which hence allows implementing the vaccination campaign into the control source patch and thus allows reducing the infectious groups and increasing the number of recovered individuals in the target patch with an optimal cost. The optimal control problem was the subject of an optimization criterion represented by the minimization of an objective function. The optimality systems are solved based on an iterative discrete scheme that converges following an appropriate test similar to the one related to the Forward-Backward Sweep Method (FBSM).

The paper is organized as follows: In section 2, the model is described. In section 3, we give some results concerning the existence of the optimal control, and we use a discrete version of Pontryagin's Maximum Principle, to investigate the necessary condition for the optimal control. The analysis of the optimal control problem and numerical simulations are given in Section 4. Finally, we conclude the paper in Section 5.

2. MODEL DESCRIPTION

Consider a discrete-time SIR model modeling the spread of an epidemic within a domain Ω , occupied by an homogeneous population, that is divided to M^2 cells uniform in size, i.e. $\Omega = \bigcup_{p,q=1,\dots,M} C_{pq}$, where C_{pq} denoting a spatial location in Ω . The spread dynamics of an infectious disease is characterized by modeling population movements between those cells (neighborhoods, towns, cities, countries...).

According to the disease transmission mechanism, the host population of each cell C_{pq} is grouped into three epidemiological compartments, $S_i^{C_{pq}}$ susceptible individuals, $I_i^{C_{pq}}$ infected individuals and $R_i^{C_{pq}}$ removed individuals, where the index i represents the time. We assume that the susceptible individuals of C_{pq} not yet infected but can be infected only through contacts with infective of C_{pq} and its neighborhood V_{pq} , where $V_{pq} = \{C_{rs} \in \Omega / r = p + k, s = q + k', k, k' \in \{-1, 0, 1\}\}$, which is a Moor neighborhood type, see Figure 1 (a).

Thus, the infection transmission at time i is assumed to be occur between individuals present in a given cell C_{pq} at rate:

$$\sum_{C_{rs} \in V_{pq}} \beta_{rs} I_i^{C_{rs}} S_i^{C_{pq}}$$

where β_{rs} is the proportion of adequate contacts between a susceptible from a cell C_{pq} and an infective from its neighbor cell $C_{rs} \in V_{pq}$, which is a constant.

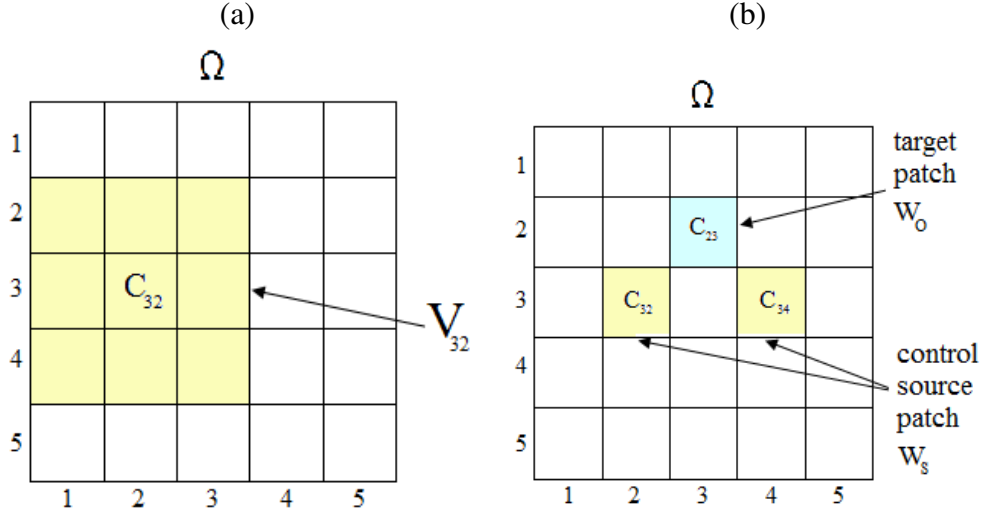
At time i , movements of susceptible, infected and removed people are also considered and occurred , respectively, at rate:

$$\begin{aligned} & \sum_{C_{rs} \in V'_{pq}} v_{rs}^S S_i^{C_{rs}} \\ & \sum_{C_{rs} \in V'_{pq}} v_{rs}^I I_i^{C_{rs}} \\ & \sum_{C_{rs} \in V'_{pq}} v_{rs}^R R_i^{C_{rs}} \end{aligned}$$

where $V'_{pq} = V_{pq} \setminus \{C_{pq}\}$, v_{rs}^S , v_{rs}^I and v_{rs}^R are the proportions of susceptible, infected and removed people coming from the neighboring cell $C_{rs} \in V'_{pq}$, respectively.

The following system describes the multi-cells discrete SIR model corresponding to a cell C_{pq} in Ω

FIGURE 1. Grid of Ω , (a) The Neighborhood V_{32} of the cell C_{32} . (b) Target patch $W_O = \{C_{23}\}$ and the control source patch $W_S = \{C_{32}, C_{34}\}$.



$$(1) \quad S_{i+1}^{C_{pq}} = S_i^{C_{pq}} - \sum_{C_{rs} \in V_{pq}} \beta_{rs} I_i^{C_{rs}} S_i^{C_{pq}} - d S_i^{C_{pq}} + \sum_{C_{rs} \in V'_{pq}} v_{rs}^S S_i^{C_{rs}} - \gamma^S S_i^{C_{pq}}$$

$$(2) \quad I_{i+1}^{C_{pq}} = I_i^{C_{pq}} + \sum_{C_{rs} \in V_{pq}} \beta_{rs} I_i^{C_{rs}} S_i^{C_{pq}} + \sum_{C_{rs} \in V'_{pq}} v_{rs}^I I_i^{C_{rs}} - (\alpha + \gamma^I + d + \gamma) I_i^{C_{pq}}$$

$$(3) \quad R_{i+1}^{C_{pq}} = R_i^{C_{pq}} + \gamma I_i^{C_{pq}} - d R_i^{C_{pq}} + \sum_{C_{rs} \in V'_{pq}} v_{rs}^R R_i^{C_{rs}} - \gamma^R R_i^{C_{pq}}$$

$S_0^{C_{pq}}$, $I_0^{C_{pq}}$ and $R_0^{C_{pq}}$ are given.

For $p, q = 1, \dots, M, d > 0$ is the natural death rate, $\alpha > 0$ is the death rate due to the infection, $\gamma > 0$ denotes the natural recovery rate of infective. By assuming that Ω is occupied by an homogeneous population, α, d and γ are assumed to be the same for all cells of Ω . Parameters description and values are given in table 1.

3. AN OPTIMAL CONTROL PROBLEM

We are interested in controlling a sensitive population (political, rich or diplomatic people or any kind of population that can be considered as an important part of society) located in a target patch denoted W_O , by following controls strategies in its neighboring cells which belong to the control source patch denoted W_S (see Figure 1 (b), for instance). For that, we introduce a control variable $u_i^{C_{rs}}$ ($C_{rs} \in W_S$) that characterizes the effectiveness of treatment (vaccination) in the above mentioned model (1-3), corresponding to cells in the control source patch W_S . Then, for a given region $C_{pq} \in \Omega$ the model is given by the following equations:

$$\begin{aligned} S_{i+1}^{C_{pq}} &= S_i^{C_{pq}} - \sum_{C_{rs} \in V_{pq}} \beta_{rs} I_i^{C_{rs}} S_i^{C_{pq}} - d S_i^{C_{pq}} + \sum_{C_{rs} \in V'_{pq}} v_{rs}^S S_i^{C_{rs}} - \\ &\gamma^S S_i^{C_{pq}} - u_i^{C_{pq}} S_i^{C_{pq}} \mathbb{1}_{W_S}(C_{pq}) \end{aligned} \quad (4)$$

$$\begin{aligned} I_{i+1}^{C_{pq}} &= I_i^{C_{pq}} + \sum_{C_{rs} \in V_{pq}} \beta_{rs} I_i^{C_{rs}} S_i^{C_{pq}} + \sum_{C_{rs} \in V'_{pq}} v_{rs}^I I_i^{C_{rs}} - \\ &(\alpha + \gamma^I + d + \gamma) I_i^{C_{pq}} \end{aligned} \quad (5)$$

$$\begin{aligned} R_{i+1}^{C_{pq}} &= R_i^{C_{pq}} + \gamma I_i^{C_{pq}} - d R_i^{C_{pq}} + \sum_{C_{rs} \in V'_{pq}} v_{rs}^R R_i^{C_{rs}} - \gamma^R R_i^{C_{pq}} + \\ &u_i^{C_{pq}} S_i^{C_{pq}} \mathbb{1}_{W_S}(C_{pq}). \end{aligned} \quad (6)$$

$S_0^{C_{pq}}$, $I_0^{C_{pq}}$ and $R_0^{C_{pq}}$ are given.

Our goal is to determine a control in the control source patch W_S which enable to minimize the infected individuals and increase the number of recovered individuals in a target patch W_O . Then, for an initial state $(S_0^{C_{pq}}, I_0^{C_{pq}}, R_0^{C_{pq}})$, $C_{pq} \in \Omega$, the problem is to minimize the objective functional given by

$$\begin{aligned} J_W(u) &= \sum_{C_{rs} \in W_O} (A_1 I_N^{C_{rs}} - A_2 R_N^{C_{rs}}) \\ &+ \sum_{i=0}^{N-1} \left(\sum_{C_{rs} \in W_O} (A_1 I_i^{C_{rs}} - A_2 R_i^{C_{rs}}) + \sum_{C_{rs} \in W_S} \frac{A_{rs}}{2} (u_i^{C_{rs}})^2 \right) \end{aligned} \quad (7)$$

where $W = W_S \cup W_O$, $u = (u^{C_{rs}})_{C_{rs} \in W_S}$, $A_{rs} > 0$, $A_1 > 0$ and $A_2 > 0$ are the weight constants of controls, the infected and the removed group respectively. This optimization is taken over a finite time horizon N because the treatment (vaccination) period is usually restricted to a limited

time window.

To clarify, that minimization is taken over a controls set,

$$(8) \quad U_{ad} = \{u \text{ measurable} / u^{min} \leq u_i^{C_{rs}} \leq u^{max}, \\ i = 0, \dots, N-1, C_{rs} \in W_S\}.$$

In other words, we are seeking an optimal control u^* such that

$$J_W(u^*) = \min\{J_W(u) / u \in U_{ad}\}.$$

The sufficient condition for existence of an optimal control for such problems follows from theorem 1 in [25]. At the same time by using a discrete version of Pontryagin's Maximum Principle [28, 29] we derive necessary conditions for our optimal control. For this purpose we define the Hamiltonian as:

$$\begin{aligned} H(\Omega) &= \sum_{C_{rs} \in W_O} (A_1 I_i^{C_{rs}} - A_2 R_i^{C_{rs}}) + \sum_{C_{rs} \in W_S} \frac{A_{rs}}{2} (u_i^{C_{rs}})^2 \\ &+ \sum_{C_{pq} \in W} \left[\zeta_{1,i+1}^{C_{pq}} \left[S_i^{C_{pq}} - \sum_{C_{rs} \in V'_{pq}} \beta_{rs} I_i^{C_{rs}} S_i^{C_{pq}} \right. \right. \\ &\quad \left. \left. - d S_i^{C_{pq}} + \sum_{C_{rs} \in V'_{pq}} v_{rs}^S S_i^{C_{rs}} - \gamma^S S_i^{C_{pq}} - u^{C_{pq}} S_i^{C_{pq}} \mathbb{1}_{W_S}(C_{pq}) \right] \right] \\ &+ \zeta_{2,i+1}^{C_{pq}} \left[I_i^{C_{pq}} + \sum_{C_{rs} \in V_{pq}} \beta_{rs} I_i^{C_{rs}} S_i^{C_{pq}} + \sum_{C_{rs} \in V'_{pq}} v_{rs}^I I_i^{C_{rs}} \right. \\ &\quad \left. - (\alpha + \gamma^I + d + \gamma) I_i^{C_{pq}} \right] \\ &+ \zeta_{3,i+1}^{C_{pq}} \left[R_i^{C_{pq}} + \gamma^I I_i^{C_{pq}} - d R_i^{C_{pq}} + \sum_{C_{rs} \in V'_{pq}} v_{rs}^R R_i^{C_{rs}} - \gamma^R R_i^{C_{pq}} + \right. \\ &\quad \left. u^{C_{pq}} S_i^{C_{pq}} \mathbb{1}_{W_S}(C_{pq}) \right] \end{aligned}$$

where $\zeta_{1,i}^{C_{pq}}$, $\zeta_{2,i}^{C_{pq}}$ and $\zeta_{3,i}^{C_{pq}}$ ($i = 0, \dots, N$) are the adjoint functions to be determined suitably.

Theorem 1. Given an optimal control u^* and solutions $S^{C_{pq}^*}$, $I^{C_{pq}^*}$ and $R^{C_{pq}^*}$, there exists $\zeta_{k,i}^{C_{pq}}$, $i = 0 \dots N$, $k = 1, 2, 3$, the adjoint variables satisfying the following equations

For $C_{pq} \in W_O$:

$$\begin{aligned}
 \Delta \zeta_{1,i}^{C_{pq}} &= - \left[(1-d-\gamma^S) \zeta_{1,i+1}^{C_{pq}} + \sum_{C_{rs} \in V_{pq}} \beta_{rs} I_i^{C_{rs}} (\zeta_{2,i+1}^{C_{pq}} - \zeta_{1,i+1}^{C_{pq}}) \right. \\
 (9) \quad &\quad \left. + \sum_{C_{rs} \in V_{pq} \cap W} v_{pq}^S \zeta_{1,i+1}^{C_{rs}} \right] \\
 \Delta \zeta_{2,i}^{C_{pq}} &= - \left[A_1 + \sum_{C_{rs} \in V_{pq} \cap W} \beta_{pq} S_i^{C_{rs}} (\zeta_{2,i+1}^{C_{rs}} - \zeta_{1,i+1}^{C_{rs}}) + \sum_{C_{rs} \in V_{pq} \cap W} v_{pq}^I \zeta_{2,i+1}^{C_{rs}} \right. \\
 (10) \quad &\quad \left. + (1 - (\alpha + \gamma^I + d + \gamma)) \zeta_{2,i+1}^{C_{pq}} + \gamma \zeta_{3,i+1}^{C_{pq}} \right] \\
 \Delta \zeta_{3,i}^{C_{pq}} &= - \left[-A_2 + (1-d-\gamma^R) \zeta_{3,i+1}^{C_{pq}} + \sum_{C_{rs} \in V_{pq} \cap W} v_{pq}^R \zeta_{3,i+1}^{C_{rs}} \right]
 \end{aligned}$$

where $\zeta_{1,N}^{C_{pq}} = 0, \zeta_{2,N}^{C_{pq}} = A_1^{pq}, \zeta_{3,N}^{C_{pq}} = -A_2^{pq}$, are the transversality conditions.
 For $C_{pq} \in W_S$:

$$\begin{aligned}
 \Delta \zeta_{1,i}^{C_{pq}} &= - \left[(1-d-\gamma^S) \zeta_{1,i+1}^{C_{pq}} + \sum_{C_{rs} \in V_{pq}} \beta_{rs} I_i^{C_{rs}} (\zeta_{2,i+1}^{C_{pq}} - \zeta_{1,i+1}^{C_{pq}}) \right. \\
 (12) \quad &\quad \left. + \sum_{C_{rs} \in V_{pq} \cap W} v_{pq}^S \zeta_{1,i+1}^{C_{rs}} + u_i^{C_{pq}} (\zeta_{3,i+1}^{C_{pq}} - \zeta_{1,i+1}^{C_{pq}}) \right] \\
 \Delta \zeta_{2,i}^{C_{pq}} &= - \left[\sum_{C_{rs} \in V_{pq} \cap W} \beta_{pq} S_i^{C_{rs}} (\zeta_{2,i+1}^{C_{rs}} - \zeta_{1,i+1}^{C_{rs}}) + \sum_{C_{rs} \in V_{pq} \cap W} v_{pq}^I \zeta_{2,i+1}^{C_{rs}} \right. \\
 (13) \quad &\quad \left. + (1 - (\alpha + \gamma^I + d + \gamma)) \zeta_{2,i+1}^{C_{pq}} + \gamma \zeta_{3,i+1}^{C_{pq}} \right] \\
 \Delta \zeta_{3,i}^{C_{pq}} &= - \left[(1-d-\gamma^R) \zeta_{3,i+1}^{C_{pq}} + \sum_{C_{rs} \in V_{pq} \cap W} v_{pq}^R \zeta_{3,i+1}^{C_{rs}} \right]
 \end{aligned}$$

where $\zeta_{1,N}^{C_{pq}} = 0, \zeta_{2,N}^{C_{pq}} = 0, \zeta_{3,N}^{C_{pq}} = 0$, are the transversality conditions. In addition for $C_{pq} \in W_S$

$$\begin{aligned}
 (15) \quad u_i^{C_{pq}^*} &= \min \left\{ \max \left\{ u^{min}, \frac{(\zeta_{1,i+1}^j - \zeta_{3,i+1}^j) S_i^{C_{pq}^*}}{A_{pq}} \right\}, u^{max} \right\}, \\
 &\quad i = 0, \dots, N-1.
 \end{aligned}$$

Proof. To proof the previous statements, we use a discrete version of Pontryagin’s Maximum Principle [28, 29] and setting $S^{C_{pq}^*}, I^{C_{pq}^*}$ and $R^{C_{pq}^*}$ and u^* we obtain the following adjoint equations:

For $C_{pq} \in W_O$:

$$\begin{aligned}\Delta \zeta_{1,i}^{C_{pq}} &= -\frac{\partial H}{\partial S_i^{C_{pq}}} = -\left[(1-d-\gamma^S) \zeta_{1,i+1}^{C_{pq}} + \sum_{C_{rs} \in V_{pq}} \beta_{rs} I_i^{C_{rs}} (\zeta_{2,i+1}^{C_{pq}} - \zeta_{1,i+1}^{C_{pq}}) \right. \\ &\quad \left. + \sum_{C_{rs} \in V_{pq} \cap W} v_{pq}^S \zeta_{1,i+1}^{C_{rs}} \right] \\ \Delta \zeta_{2,i}^{C_{pq}} &= -\frac{\partial H}{\partial I_i^{C_{pq}}} = -\left[A_1 + \sum_{C_{rs} \in V_{pq} \cap W} \beta_{pq} S_i^{C_{rs}} (\zeta_{2,i+1}^{C_{rs}} - \zeta_{1,i+1}^{C_{rs}}) \right. \\ &\quad \left. + \sum_{C_{rs} \in V_{pq} \cap W} v_{pq}^I \zeta_{2,i+1}^{C_{rs}} + (1-(\alpha+\gamma^I+d+\gamma)) \zeta_{2,i+1}^{C_{pq}} + \gamma \zeta_{3,i+1}^{C_{pq}} \right] \\ \Delta \zeta_{3,i}^{C_{pq}} &= -\frac{\partial H}{\partial R_i^{C_{pq}}} = -\left[-A_2 + (1-d-\gamma^R) \zeta_{3,i+1}^{C_{pq}} + \sum_{C_{rs} \in V_{pq} \cap W} v_{pq}^R \zeta_{3,i+1}^{C_{rs}} \right]\end{aligned}$$

with transversality conditions

$$\zeta_{1,N}^{C_{pq}} = 0, \zeta_{2,N}^{C_{pq}} = A_1^{pq}, \zeta_{3,N}^{C_{pq}} = -A_2^{pq}$$

and

for $C_{pq} \in W_S$:

$$\begin{aligned}\Delta \zeta_{1,i}^{C_{pq}} &= -\frac{\partial H}{\partial S_i^{C_{pq}}} = -\left[(1-d-\gamma^S) \zeta_{1,i+1}^{C_{pq}} + \sum_{C_{rs} \in V_{pq}} \beta_{rs} I_i^{C_{rs}} (\zeta_{2,i+1}^{C_{pq}} - \zeta_{1,i+1}^{C_{pq}}) \right. \\ &\quad \left. + \sum_{C_{rs} \in V_{pq} \cap W} v_{pq}^S \zeta_{1,i+1}^{C_{rs}} + u_i^{C_{pq}} (\zeta_{3,i+1}^{C_{pq}} - \zeta_{1,i+1}^{C_{pq}}) \right] \\ \Delta \zeta_{2,i}^{C_{pq}} &= -\frac{\partial H}{\partial I_i^{C_{pq}}} = -\left[\sum_{C_{rs} \in V_{pq} \cap W} \beta_{pq} S_i^{C_{rs}} (\zeta_{2,i+1}^{C_{rs}} - \zeta_{1,i+1}^{C_{rs}}) \right. \\ &\quad \left. + \sum_{C_{rs} \in V_{pq} \cap W} v_{pq}^I \zeta_{2,i+1}^{C_{rs}} + (1-(\alpha+\gamma^I+d+\gamma)) \zeta_{2,i+1}^{C_{pq}} + \gamma \zeta_{3,i+1}^{C_{pq}} \right] \\ \Delta \zeta_{3,i}^{C_{pq}} &= -\frac{\partial H}{\partial R_i^{C_{pq}}} = -\left[(1-d-\gamma^R) \zeta_{3,i+1}^{C_{pq}} + \sum_{C_{rs} \in V_{pq} \cap W} v_{pq}^R \zeta_{3,i+1}^{C_{rs}} \right]\end{aligned}$$

with

$$\zeta_{1,N}^{C_{pq}} = 0, \zeta_{2,N}^{C_{pq}} = 0, \zeta_{3,N}^{C_{pq}} = 0$$

To obtain the optimality conditions we take the variation with respect to control $u_i^{C_{pq}*}$ and set it equal to zero

$$\frac{\partial H}{\partial u_i^{C_{pq}}} = A_{pq} u_i^{C_{pq}} - \zeta_{1,i+1}^{C_{pq}} S_i^{C_{pq}} + \zeta_{3,i+1}^{C_{pq}} S_i^{C_{pq}} = 0.$$

Then we obtain the optimal control

$$u_i^{C_{pq}*} = \frac{(\zeta_{1,i+1}^{C_{pq}} - \zeta_{3,i+1}^{C_{pq}}) S_i^{C_{pq}}}{A_{pq}}.$$

By the bounds in U_{ad} of the control, it is easy to obtain $u_i^{C_{pq}^*}$ in the following form

$$u_i^{C_{pq}^*} = \max\left\{\min\left\{\frac{(\zeta_{1,i+1}^{C_{pq}} - \zeta_{3,i+1}^{C_{pq}})S_i^{C_{rs}}}{A_{pq}}, u_{max}\right\}, u_{min}\right\},$$

$$i = 0, \dots, N - 1$$

□

4. NUMERICAL SIMULATIONS AND DISCUSSIONS

In this section, we provide numerical simulations to demonstrate our theoretical results in the case when the studied domain represents the assembly of M^2 regions or cells (cities, towns, ...). The code is written and compiled in MATLAB using data cited in Table 1. The optimality systems are solved using an iterative method where at instant i , the states $S_i^{C_{pq}}$, $I_i^{C_{pq}}$, and $R_i^{C_{pq}}$ with an initial guess, are obtained based on a progressive scheme in time, and their adjoint variables $\zeta_{i,l}^{C_{pq}}$, $l = 1; 2; 3$ are obtained based on a regressive scheme in time because of the transversality conditions. Afterward, we update the optimal controls values (15) using the values of state and costate variables obtained in the previous steps. Finally, we execute the previous steps until a tolerance criterion is reached. In order to show the importance of our work and without loss of generality, we consider here that $M = 5$ and then we present our numerical simulations in a 5×5 grid and which represents the global domain of interest Ω .

At the initial instant $i = 0$, susceptible people are homogeneously distributed with 100 individuals in each cell except at the lower right corner cell C_{55} , where we introduce 10 infected individuals and 90 susceptible ones.

In all of the figures below, the redder part of the colorbars contains larger numbers of individuals while the bluer part contains the smaller numbers. In the following, we discuss with more details, the simulations we obtain, in the case when there is yet no control.

4.1. Simulations without controls. In this section, Figures 2., 3., and 4. depict dynamics of the susceptible, infected and removed population, respectively, in the case when there is yet no control strategy, followed for the prevention of the epidemic, and we note that in all these figures presented here, simulations give us an idea about the spread of the disease. For instance, in Figure 2, if we suppose there are 90 susceptible people in cell C_{55} located at the lower right

TABLE 1. Parameters values associated to a cell C_{pq} , $p, q = 1, \dots, M$, which utilized for the resolution of all multi-cells discrete-time systems (1)-(3) and (4)-(6), and then leading to simulations obtained from Figure 2 to Figure 10, with the initial conditions $S_0^{C_{pq}}, I_0^{C_{pq}}$ and $R_0^{C_{pq}}$ associated to any cell C_{pq} of Ω .

Parameter	Description	Value
$S_0^{C_{pq}}$	Initial value of susceptible	100
$I_0^{C_{pq}}$	Initial value of infected	0
$R_0^{C_{pq}}$	Initial value of removed	0
β_{rs}	infection transmission rate	2×10^{-5}
d	Natural death rate	1×10^{-4}
γ	Natural recovery rate	2×10^{-5}
γ^S	Exit rate of susceptibles	2×10^{-4}
γ^I	Exit rate of infecteds	1×10^{-5}
γ^R	Exit rate of removeds	2×10^{-4}
v_{rs}^S	Entry rate of susceptibles from cell C_{rs}	2×10^{-4}
v_{rs}^I	Entry rate of infecteds from cell C_{rs}	1×10^{-5}
v_{rs}^R	Entry rate of removeds from cell C_{rs}	2×10^{-4}
α	Death rate due to the infection	2×10^{-3}

corner of Ω , and 100 in each other cell, we can see that at instant $i = 300$, in most cells of Ω , $S^{C_{pq}}$ becomes more important, taking values between 120 and 150 because of movements of susceptible individuals from other regions out of Ω . At instant $i = 700$, the number $S^{C_{55}}$ becomes less important and takes a value close/or equal to 50, while $S^{C_{pq}}$ in cells of Ω starts decreasing, and as we move away from V_{55} , $S^{C_{pq}}$ remains important.

In Figure 3., if we suppose there are 10 infected people in cell C_{55} , and no infection in all other cells, we observe that at instant $i = 300$, the number $I^{C_{55}}$ starts increasing to bigger values, while $I^{C_{pq}}$ in cells of V_{55} take values close/or equal to 25, and as we move away from V_{55} , $I^{C_{pq}}$ remains less important. At instant $i = 550$, we can see that in most of cells, $I^{C_{pq}}$ becomes more important, taking values between 50 and 80 in cells which are close to cells with 8 neighboring cells, while

FIGURE 2. $S^{C_{pq}}$ behavior in the absence of optimal controls (15). The disease starts from the lower corner C_{55} .

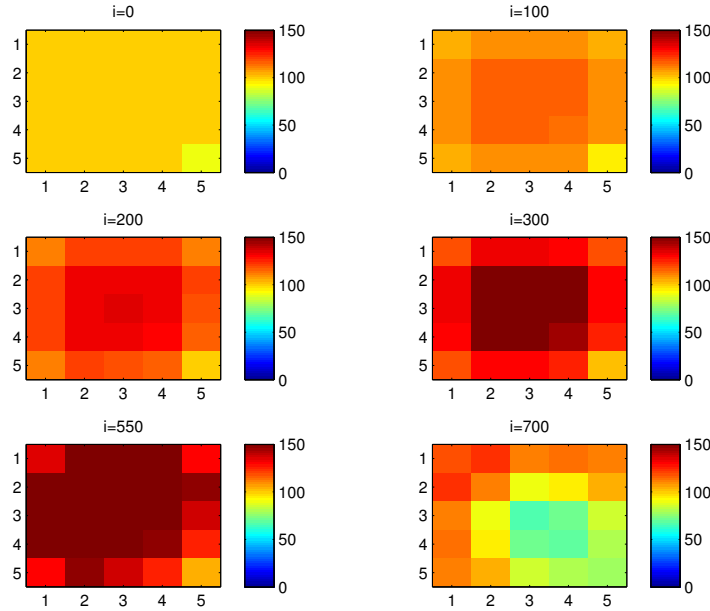
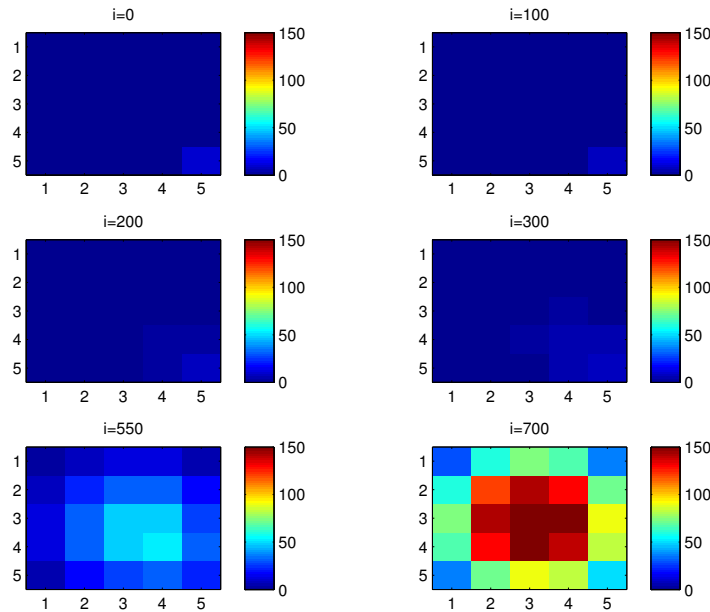
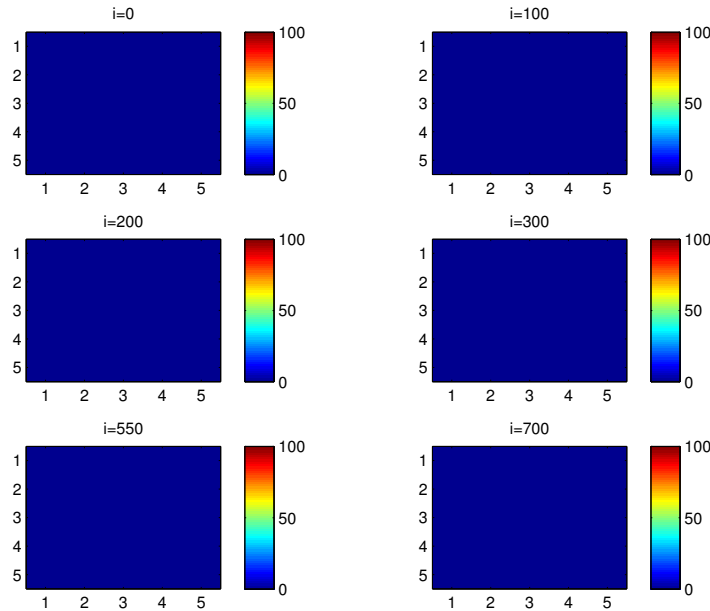


FIGURE 3. $I^{C_{pq}}$ behavior in the absence of optimal controls (15). The disease starts from the lower corner C_{55} .



in a few other cells, it takes values between 0 and 40. From these numerical results, we can deduce that once the infection arrives at the center or to the cells with 8 cells in their vicinity sets, the infection becomes more important compared to the case of the previous instant. At

FIGURE 4. $R^{C_{pq}}$ behavior in the absence of optimal controls (15). The disease starts from the lower corner C_{55} .



instant $i = 700$, $I^{C_{pq}}$ takes values close/or equal to 120 in the cell from where the epidemic has started, and 90 in V_{55} and near to it, and as we move away towards the center and further regions, infection is important with the presence of more than 130 infected individuals in each cell except the ones in the 3 opposite corners.

As we can observe in Figure 4. that the number $R^{C_{pq}}$ in all cells of Ω are close/or equal to only 1 or two removed people, some people acquire immune responses that help them to cure naturally from the disease.

4.2. Simulations with controls. Figures 5., 6., 7., 8., 9. and 10. depict dynamics of the S, I and R populations when the vaccination optimal control strategy is followed. In order to show the importance of the optimal control approach suggested in this paper, we take the example of a target cell which has 8 neighboring cells, and as done in the previous part, we investigate also here, the results obtained when the disease starts from the lower right corner. As an example, we suppose that the target patch we aim to control is $W_O = \{C_{23}\}$, the control source patch is $W_S = \{C_{32}, C_{34}\}$ and we present simulations when the epidemic is more important at the corner cell C_{55} .

FIGURE 5. $S^{C_{pq}}$ behavior in the presence of optimal controls (15) in the control source patch $W_S = \{C_{32}, C_{34}\}$. The disease starts from the lower corner C_{55} .

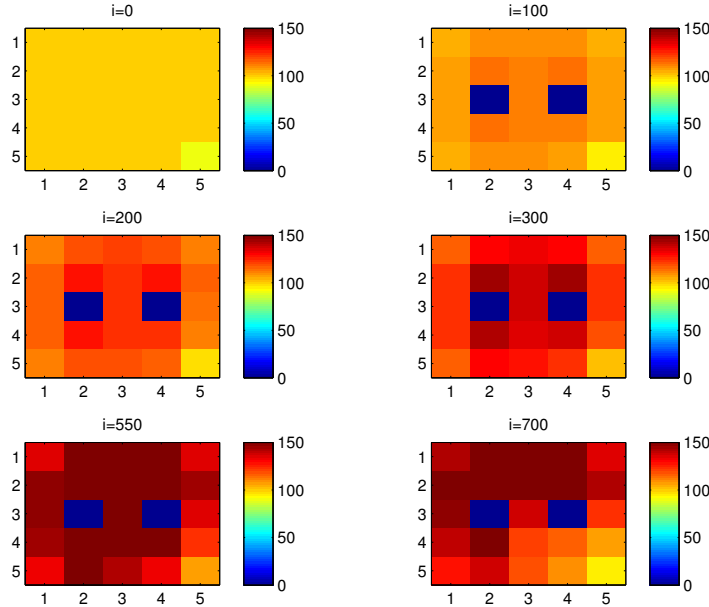
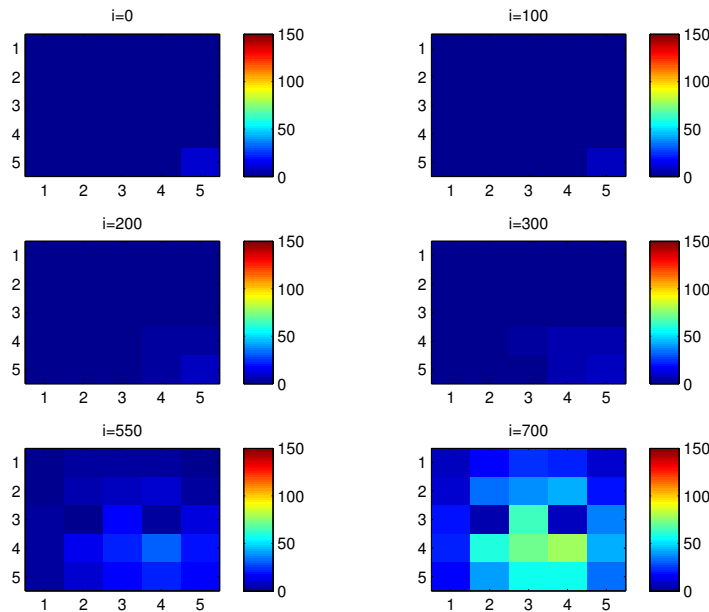


FIGURE 6. $I^{C_{pq}}$ behavior in the presence of optimal controls (15) in the control source patch $W_S = \{C_{32}, C_{34}\}$. The disease starts from the lower corner C_{55} .



In the following, we note that the vicinity of the patch W_O is defined by

$$W_O = \{C_{12}, C_{13}, C_{14}, C_{22}, C_{24}, C_{32}, C_{33}, C_{34}\}$$

FIGURE 7. $R^{C_{pq}}$ behavior in the presence of optimal controls (15) in the control source patch $W_S = \{C_{32}, C_{34}\}$. The disease starts from the lower corner C_{55} .

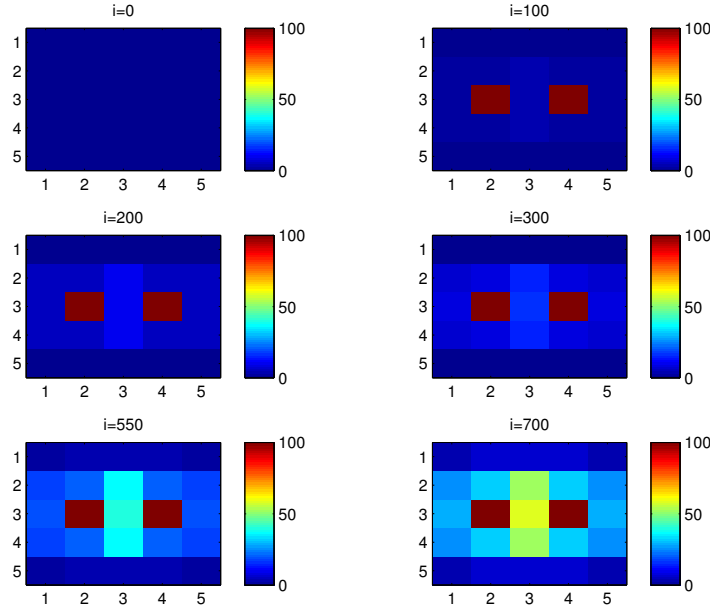


FIGURE 8. States curves in the absence of controls. (a): $S^{C_{23}}, I^{C_{23}}$ and $R^{C_{23}}$ associated to the target cell C_{23} . (b): $S^{C_{32}}, I^{C_{32}}$ and $R^{C_{32}}$ associated to the first cell C_{32} in the source control patch W_S . (c): $S^{C_{34}}, I^{C_{34}}$ and $R^{C_{34}}$ associated to the second cell C_{34} in the control source patch W_S . (d): $S^{C_{55}}, I^{C_{55}}$ and $R^{C_{55}}$ associated to the cell C_{55} the source of the disease.

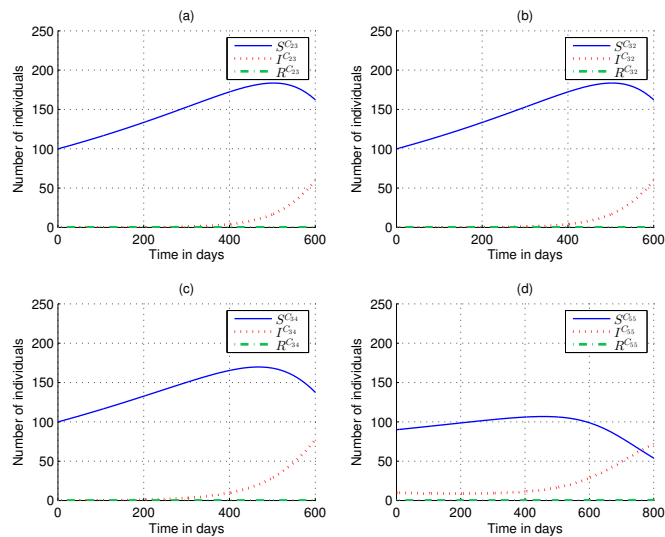


FIGURE 9. States curves in the presence of controls. (a): $S^{C_{23}}, I^{C_{23}}$ and $R^{C_{23}}$ associated to the target cell C_{23} . (b): $S^{C_{32}}, I^{C_{32}}$ and $R^{C_{32}}$ associated to the first cell C_{32} in the source control patch W_S . (c): $S^{C_{34}}, I^{C_{34}}$ and $R^{C_{34}}$ associated to the second cell C_{34} in the control source patch W_S . (d): $S^{C_{55}}, I^{C_{55}}$ and $R^{C_{55}}$ associated to the cell C_{55} the source of the disease.

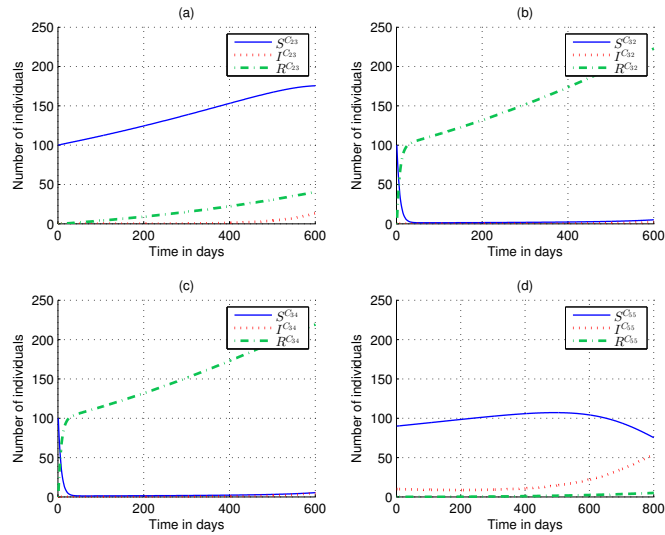
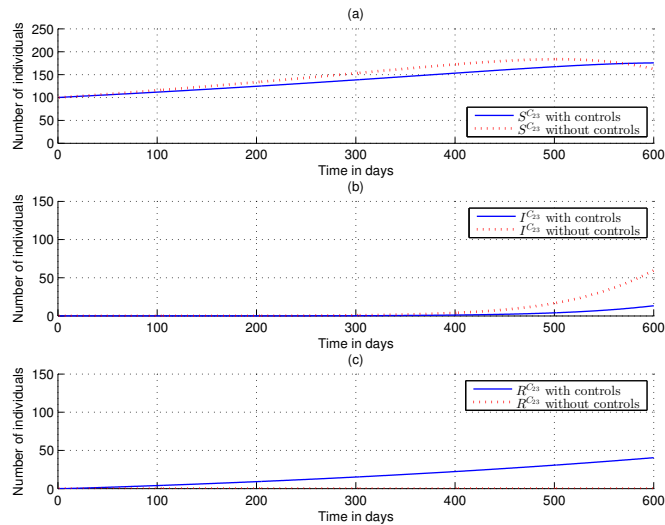


FIGURE 10. Comparison of the target cell C_{23} states with and without controls. (a) $S^{C_{23}}$ as function of time. (b) $I^{C_{23}}$ as function of time. (c) $R^{C_{23}}$ as function of time.



and the vicinity of the control source patch W_S is

$$V_{W_S} = \{C_{21}, C_{22}, C_{23}, C_{24}, C_{25}, C_{31}, C_{41}, C_{42}, C_{43}, C_{44}, C_{45}, C_{35}, C_{33}\}.$$

In Figure 5., as supposed also above, there are 90 susceptible individuals in cell C_{55} , and 100 in each other cell. We can see that at instant $i = 100$, the numbers $S^{C_{55}}$ and $S^{C_{pq}}$ are at most the same as in the case when there was no control strategy, while in the control source patch, $S^{C_{32}}$ and $S^{C_{34}}$ take almost zero values. At instant $i=700$, susceptible population start decreasing from the lower right corner where the disease has started, even at this instant, the number of susceptible people in the source control patch conserved its values.

In Figure 6., and as done in the case without controls, we can also observe that the disease spreads towards the corners and borders of Ω . For instance, at instant $i = 550$, the number of infected people has increased in the vicinity of the patch W_S and in V_{W_O} , and as more, we move away to the corners and borders, infection is still low. At instant $i = 700$, $I^{C_{pq}}$ takes more important values in most cells except at the upper corners, noting that the number of infected people in the control source patch W_S , and $I^{C_{pq}}$ in the target patch W_O , are more reduced, due to the effectiveness of optimal controls, than the case when there are no controls in Figure 3.

As regards the removed population, in Figure 7, at instant $i=100$, $R^{C_{pq}}$ in the control source patch becomes more important taking values between 100 and 150 individuals, even in the target patch W_O , compared with the case when there are no controls. At instants $i=300$, $i=350$ and $i=700$, the number of removed individuals becomes more and more important than before, and as we move away from V_{W_S} , $R^{C_{pq}}$ is still zero.

Thus, we can deduce that the vaccination optimal control strategy has proved its effectiveness earlier.

We can observe in Figure 8, the different curves of states of the target cell and the control source cells, without controls, we can see more precisely the values of each state of cells in W_O and W_S .

In Figure 9., we see that the number of the infected population has decreased importantly in the control source patch even in the target cell and the number of the removed individuals becomes more important after the introduction of the vaccination optimal control strategy, compared with results in Figure 8. We provide Figure 10 here to show the difference, after and before introducing the optimal control strategy, between states of the target cell.

The susceptible population in that figure (a), still increasing in time after using the optimal controls, while start decreasing at the instant $i=500$ before. Figure 10 (b) shows that the number of infected individuals reached a big value equal to 60 individuals at instant $i=600$, but in the presence of controls, it takes a maximum value not exceeding 20 individuals.

While the removed population retains almost zero value in the absence of controls, the number of removed individuals increases in time to a greater value towards 48 individuals at the time $i = 600$ after the introduction of the optimal vaccination control strategy, as shown in Figure 10 (c).

In Figures 5., 6. and 7., we investigate the effectiveness of the optimal vaccination control approach on the SIR populations of Ω , when it is applied to the control source patches W_S for the purpose of controlling a sensitive target patch W_O . We can see that at instant $i = 700$, the number of SIR people in the two patches satisfying the control objective, that is the minimization of the infected population and the increase of the removed one.

However, the most interesting idea we can extract from these figures, is that regardless of the position of the control source patch W_S concerning the target patch W_O , by respecting the fact $V_{W_O} \cap V_{W_S} \neq \emptyset$, the control objective is well done, and the number of susceptible people in the target patch has not decreased significantly and the number of the infected population becomes less important, and the removed one becomes huge in time.

Since when we aim to control only one cell as in the previous simulations, the vicinity set associated with this cell contains 8 cells including cells of the control source patch. Thus, for instance in the example above, it remains 6 cells, in the vicinity set of the target cell, not controlled, and then the movements of infected travelers entering from these 6 cells can increase efficiently the number of the infected individuals in that cell.

5. CONCLUSIONS

In this paper, we presented a multi-region SIR epidemic model in the discrete-time, and we investigated a neighboring infection optimal control strategies.

We presented a new epidemic modeling approach, based on dividing the studied domain to several parts called cells or regions, these cells are assembled in one grid represents the studied

domain. Two cells are neighboring in the grid, meaning that there are means of transport between them, whatever their geographical locations. In order to contribute to the improvement of the epidemic modeling and control, we considered a discrete-time multi-regions SIR epidemic model in which we have introduced also movements of susceptibles and removed people.

A new optimal control approach is investigated to characterize the treatment injected in a control source patch and which allow reducing the number of infected population and to increase the removed ones in a target patch which is considered an important class of society. A discrete version of Pontryagin's maximum principle is done to analyze the optimal control problem and numerical simulation is given to illustrate the obtained results.

CONFLICT OF INTERESTS

The author(s) declare that there is no conflict of interests.

REFERENCES

- [1] F. Brauer, C. Castillo-Chavez, C. Castillo-Chavez, *Mathematical models in population biology and epidemiology*, Vol. 2, Springer, New York, 2012.
- [2] O. Diekmann, J. A. P. Heesterbeek, *Mathematical epidemiology of infectious diseases: model building, analysis and interpretation*, Vol. 5, John Wiley & Sons, Chichester, 2000.
- [3] H. W. Hethcote, The mathematics of infectious diseases, *SIAM Rev.* 42 (4) (2000), 599–653.
- [4] S. Hsu, A. Zee, Global spread of infectious diseases, *J. Biol. Syst.* 12 (03) (2004), 289–300.
- [5] H. R. Joshi, S. Lenhart, M. Y. Li, L. Wang, Optimal control methods applied to disease models, *Contemp. Math.* 410 (2006), 187–208.
- [6] S. Ruan, W. Wang, Dynamical behavior of an epidemic model with a nonlinear incidence rate, *J. Differ. Equ.* 188 (1) (2003), 135–163.
- [7] H. R. Joshi, Optimal control of an hiv immunology model, *Opt. Control Appl. Meth.* 23 (4) (2002), 199–213.
- [8] O. Zakary, M. Rachik, I. Elmouki, A multi-regional epidemic model for controlling the spread of Ebola: awareness, treatment, and travel-blocking optimal control approaches. *Math. Meth. Appl. Sci.* 40 (2017), 1265–1279.
- [9] C. Bekoe, The sir model and the 2014 ebola virus disease outbreak in guinea, liberia and sierra leone, *Int. J. Appl. Sci.* 6 (2) (2015), 11-24.

- [10] S. Baize, D. Pannetier, L. Oestereich, T. Rieger, L. Koivogui, N. Magassouba, B. Soropogui, M. S. Sow, S. Keïta, H. De Clerck, et al., Emergence of zaire ebola virus disease in guinea, *N. Engl. J. Med.* 371 (15) (2014), 1418–1425.
- [11] J. P. Tian, J. Wang, Global stability for cholera epidemic models, *Math. Biosci.* 232 (1) (2011), 31–41.
- [12] G. Wanner, E. Hairer, Solving ordinary differential equations II, Springer Berlin Heidelberg, 1996.
- [13] S. Liao, J. Wang, Stability analysis and application of a mathematical cholera model, *Math. Biosci. Eng.* 8 (3) (2011), 733–752.
- [14] O. Prosper, N. Ruktanonchai, M. Martcheva, Optimal vaccination and bednet maintenance for the control of malaria in a region with naturally acquired immunity, *J. Theor. Biol.* 353 (2014), 142–156.
- [15] B. N. Kim, K. Nah, C. Chu, S. U. Ryu, Y. H. Kang, Y. Kim, Optimal control strategy of plasmodium vivax malaria transmission in korea, *Osong Public Health Res. Perspect.* 3 (3) (2012), 128–136.
- [16] F. Agosto, Optimal isolation control strategies and cost-effectiveness analysis of a two-strain avian influenza model, *Biosystems.* 113 (3) (2013), 155–164.
- [17] J. Arino, F. Brauer, P. Van Den Driessche, J. Watmough, J. Wu, A model for influenza with vaccination and antiviral treatment, *J. Theor. Biol.* 253 (1) (2008), 118–130.
- [18] B. Sara, Z. Omar, T. Abdessamad, R. Mostafa, F. Hanane, Parameters' estimation, sensitivity analysis and model uncertainty for an influenza a mathematical model: case of morocco, *Commun. Math. Biol. Neurosci.* 2020 (2020), Article ID 57.
- [19] M. Lhous, O. Zakary, M. Rachik, E. M. Magri, A. Tridane, Optimal containment control strategy of the second phase of the covid-19 lockdown in morocco, *Appl. Sci.* 10 (21) (2020), 7559.
- [20] O. Zakary, S. Bidah, M. Rachik, The impact of staying at home on controlling the spread of covid-19: Strategy of control, *Mexican J. Biomed. Eng.* 42 (1) (2021), 10–26.
- [21] O. Zakary, S. Bidah, M. Rachik, H. Ferjouchia, Mathematical model to estimate and predict the covid-19 infections in morocco: Optimal control strategy, *J. Appl. Math.* 2020 (2020), 9813926.
- [22] S. Bidah, O. Zakary, M. Rachik, Modeling and control of the public opinion: An agree-disagree opinion model, *Int. J. Differ. Equ.* 2020 (2020), 5864238.
- [23] B. Hamza, B. Sara, Z. Omar, A. Imane, R. Mostafa, New automated optimal vaccination control with a multi-region sirs epidemic mode, *Commun. Math. Biol. Neurosci.* 2020 (2020), Article ID 70.
- [24] L. J. Allen, Some discrete-time si, sir, and sis epidemic models, *Math. Biosci.* 124 (1) (1994), 83–105.
- [25] K. Dabbs, Optimal control in discrete pest control models, *Optimal control in discrete pest control models.* University of Tennessee Honors Thesis Projects, 2010.
- [26] Y. Enatsu, Y. Nakata, Y. Muroya, Global stability for a class of discrete sir epidemic models, *Math. Biosci. Eng.* 7 (2) (2010), 347–361.

- [27] X. Ma, Y. Zhou, H. Cao, Global stability of the endemic equilibrium of a discrete sir epidemic model, *Advances in Difference Equations*, 2013 (2013), 42.
- [28] L. S. Pontryagin, *Mathematical theory of optimal processes*, CRC Press, Boca Raton, 1987.
- [29] S. P. Sethi, G. L. Thompson, *What is optimal control theory?*, Springer, New York, 2000.